Radioloudness of Active Galaxies and the Black Hole Evolution

Marek Sikora

(with Lukasz Stawarz and Jean-Pierre Lasota)

Trzebieszowice Castle, 2007

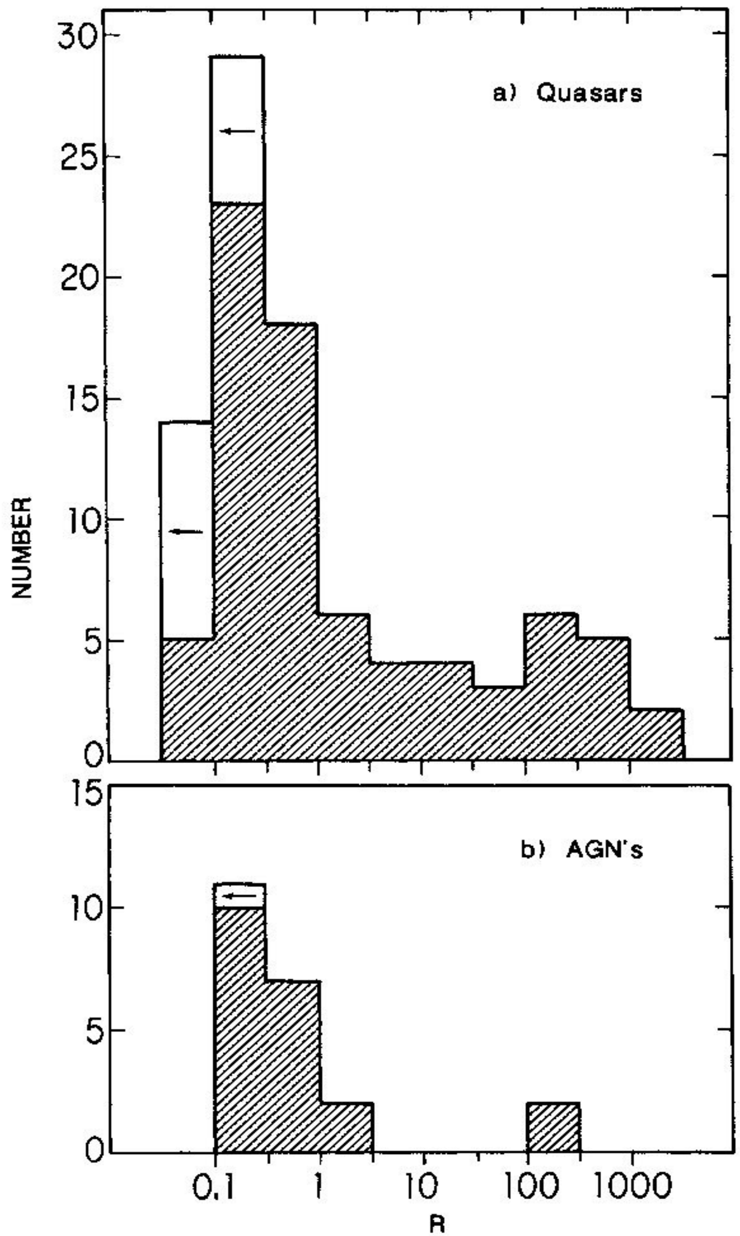

FIG. 5. Distribution of R for (a) 91 quasars in the BQS sample and (b) the 22 AGNs.

$$\mathcal{R} \equiv L_{\nu_R}/L_{\nu_O}$$

$$L_R \equiv \nu_R L_{\nu_R},\ L_O \equiv \nu_O L_{\nu_O}$$

$$L_R/L_O \sim 10^{-5}\mathcal{R}$$

Kellermann et al. '89

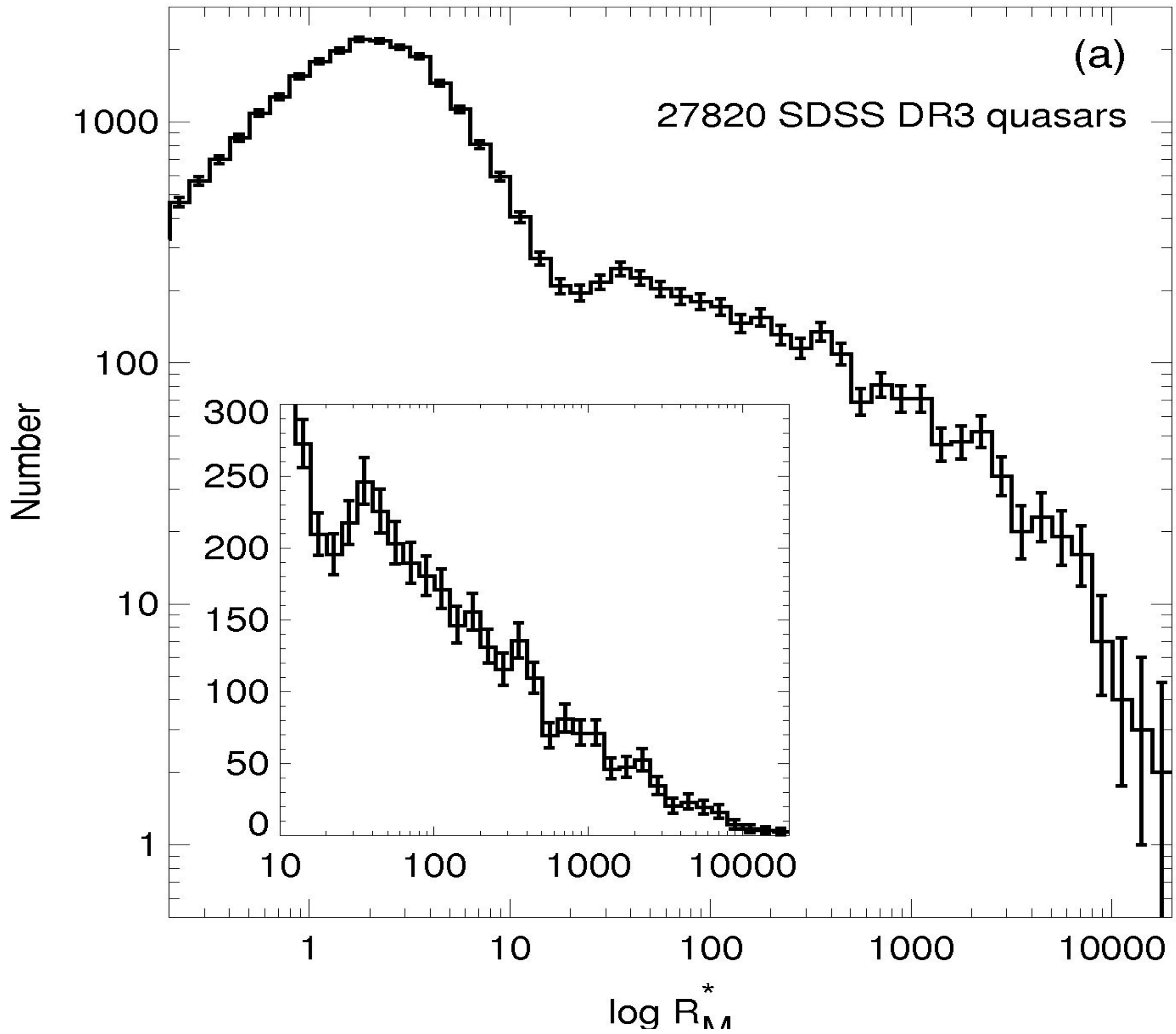

White et al. '07

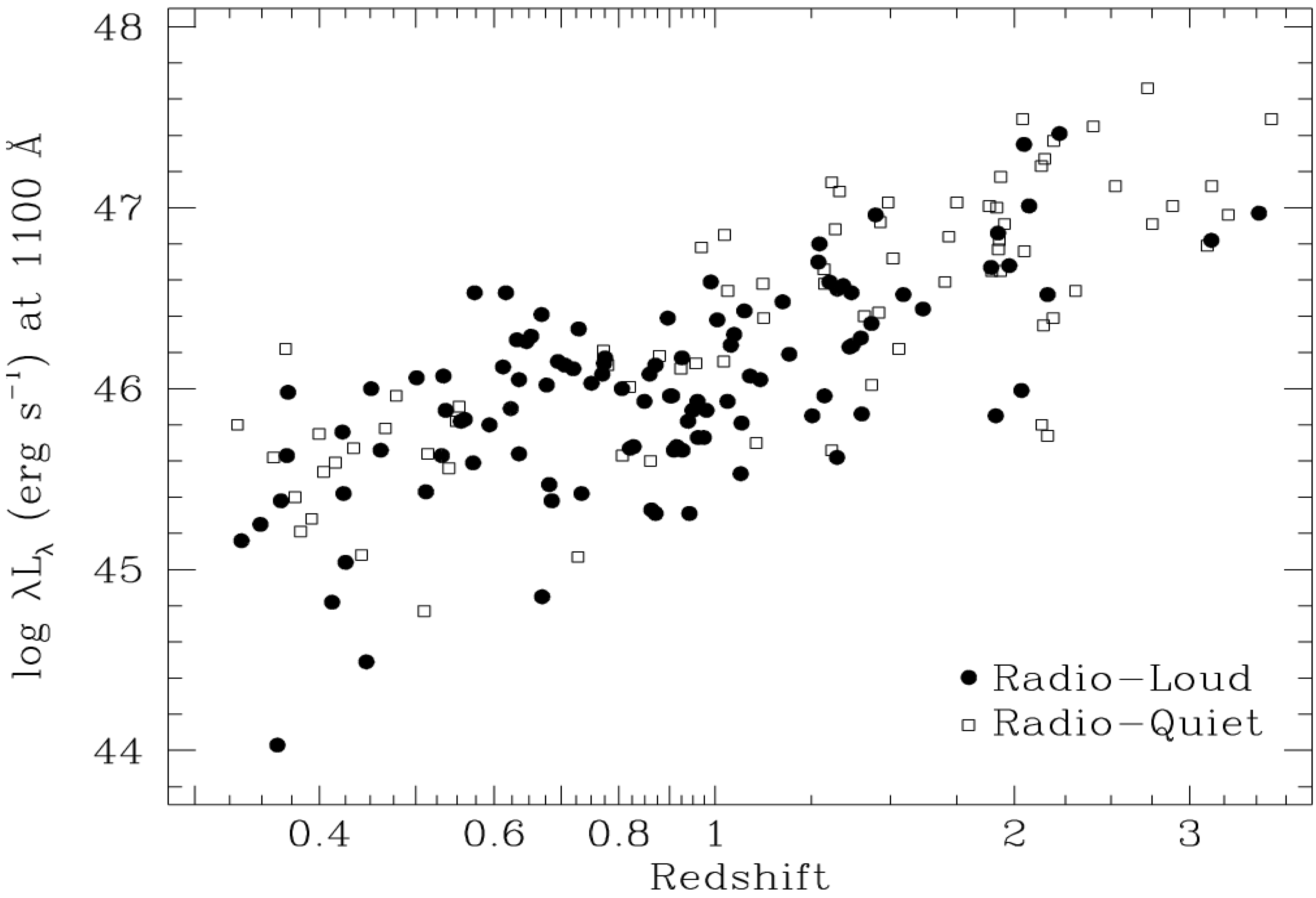

Telfer et al. '02

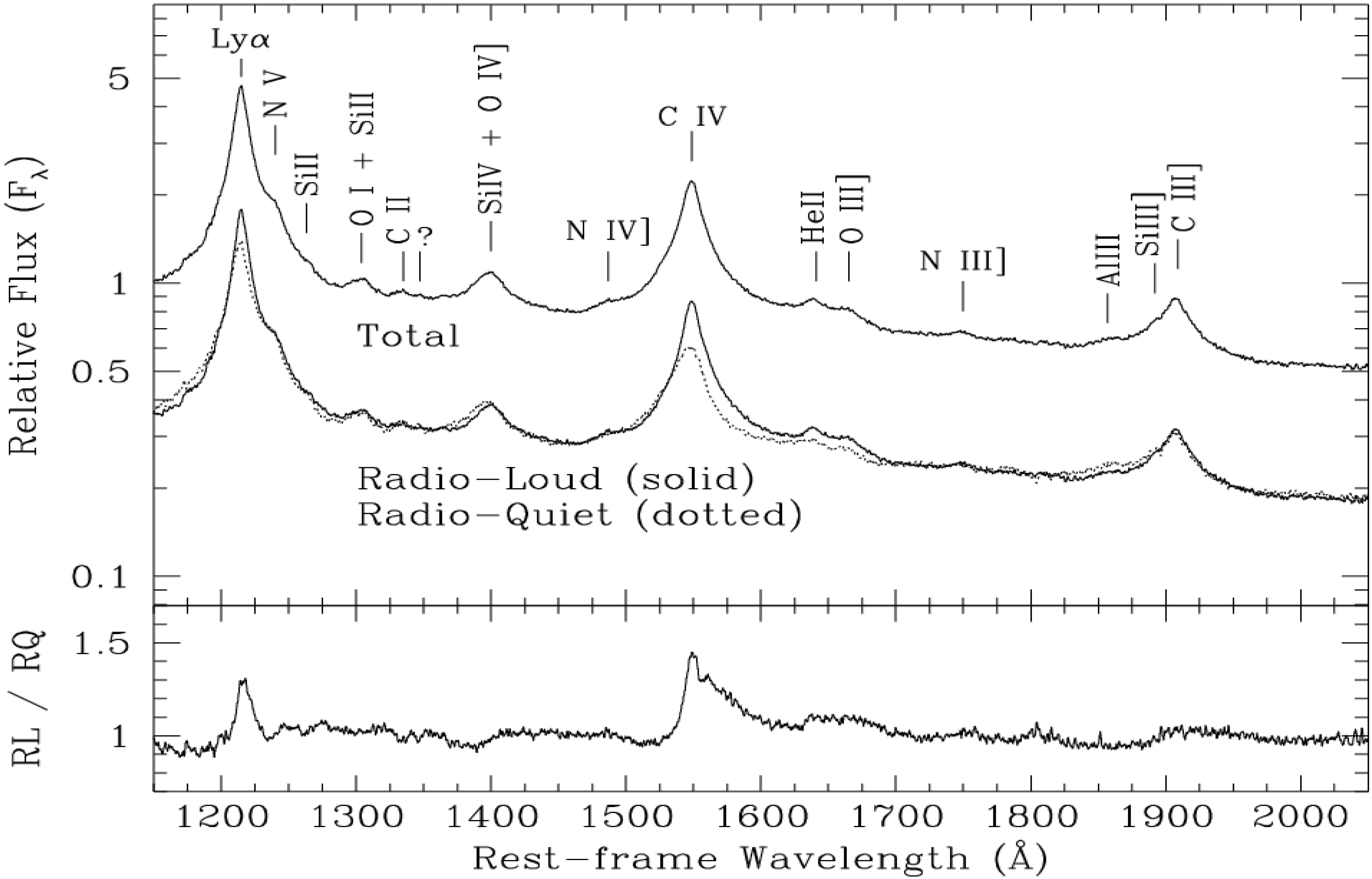

Telfer et al. '02

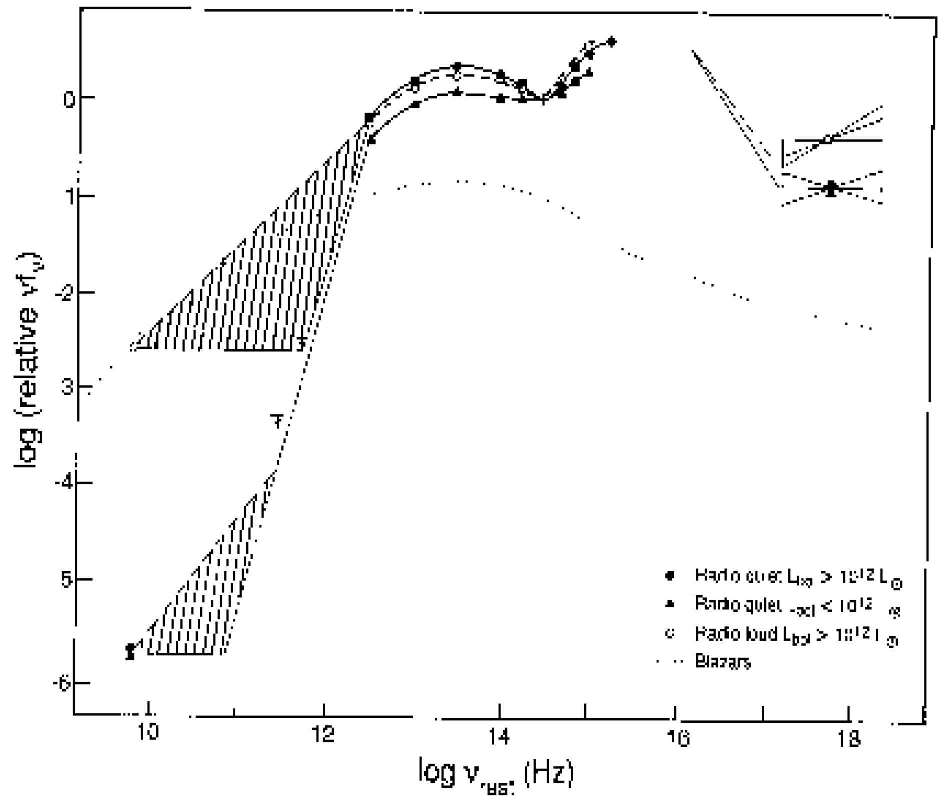

FIG. 2.—Average continuum energy distributions for radio-loud and radio-quiet PG quasars. The data points are mean values for the quasars in Fig. 1. Variations in the mean are typically 0.15 in the log for the far infrared data, and 0.1 in the log for the near-infrared and optical data. The X-ray slopes are adopted from Wilkes and Elvis (1987). The hatched region at radio-submillimeter wavelengths represents the range of spectral indices observed. Shown for comparison (*dotted line*) is the mean continuum energy distribution for blazars (Impey and Neugebauer 1988), normalized at 6 cm (see text).

Sanders et al. '89

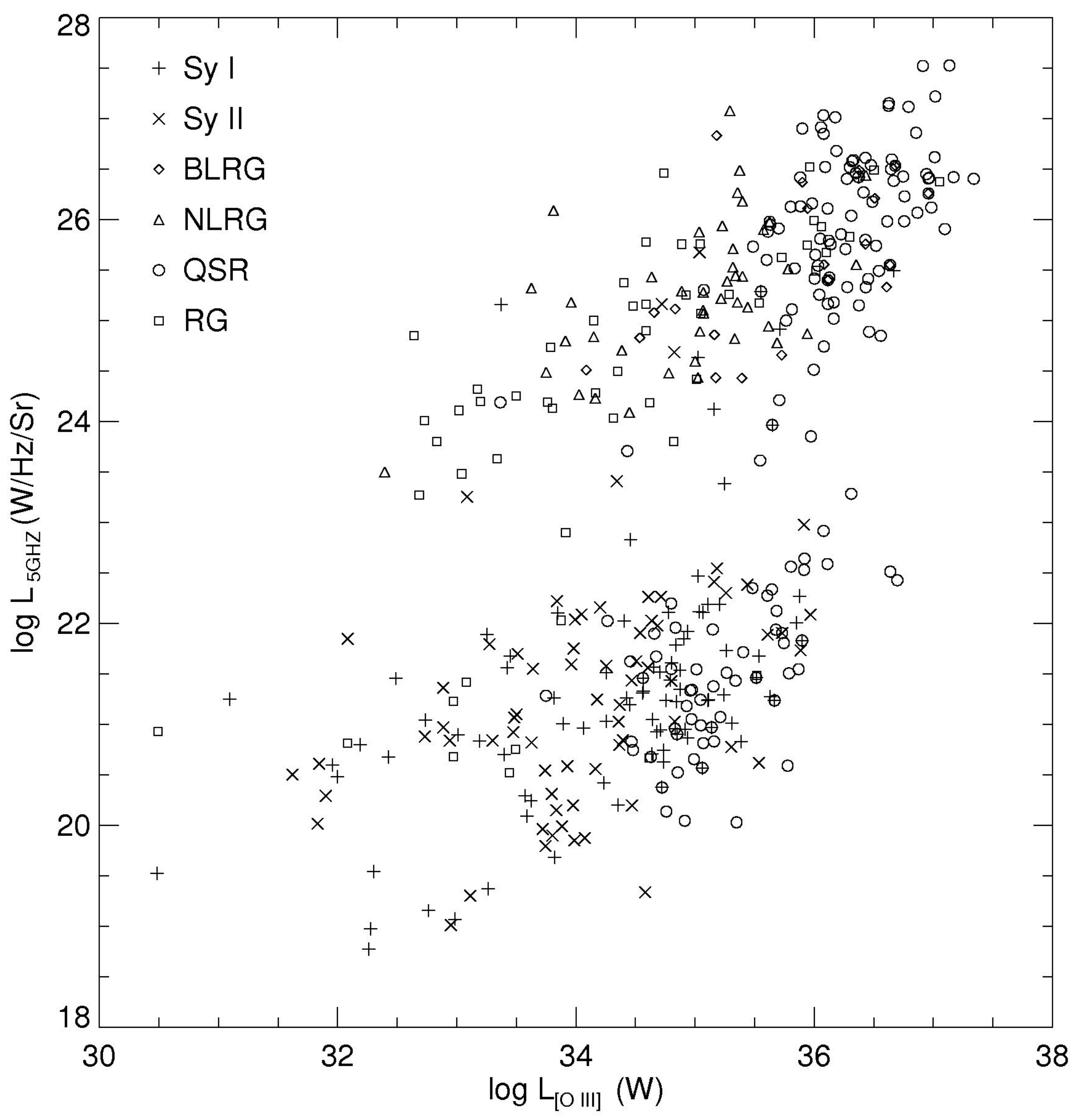
28
26
24
22
20
18
30
32
34
36
38
Sy I
Sy II
BLRG
NLRG
QSR
RG
log L5GHZ (W/Hz/Sr)
log L[O III] (W)

Xu et al. '99

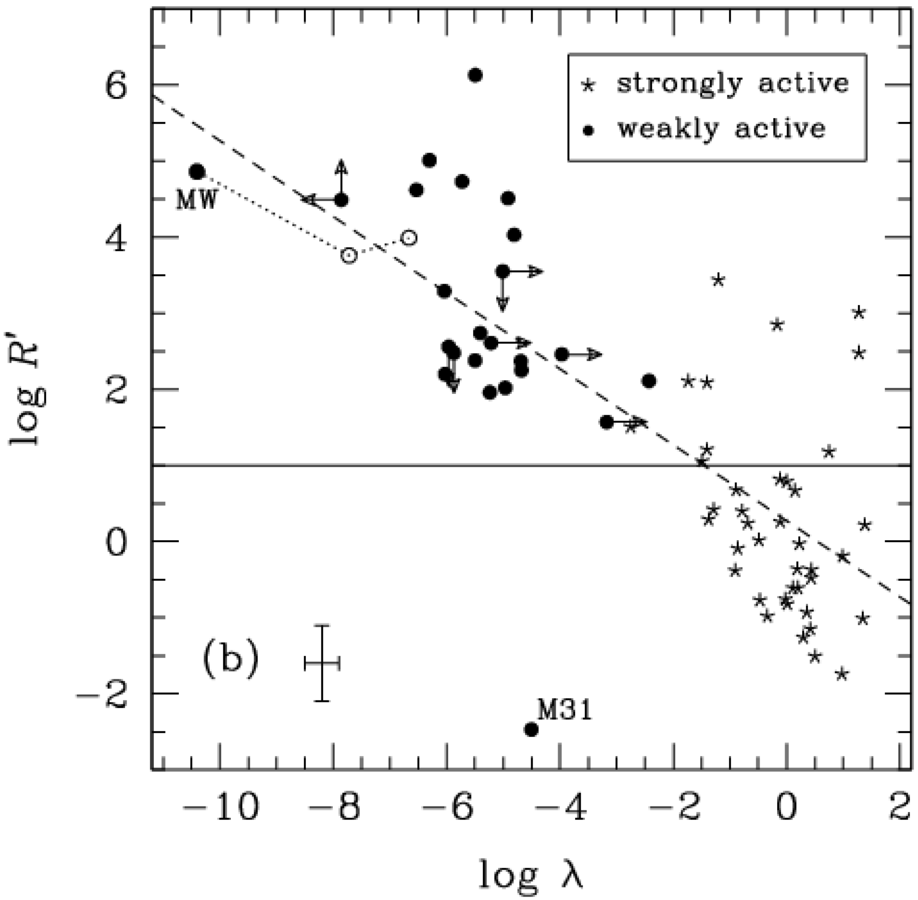
strongly active
weakly active
MW
M31
(b)
6
4
2
0
−2
−10
−8
−6
−4
−2
0
2
log R′
log λ

Ho '02

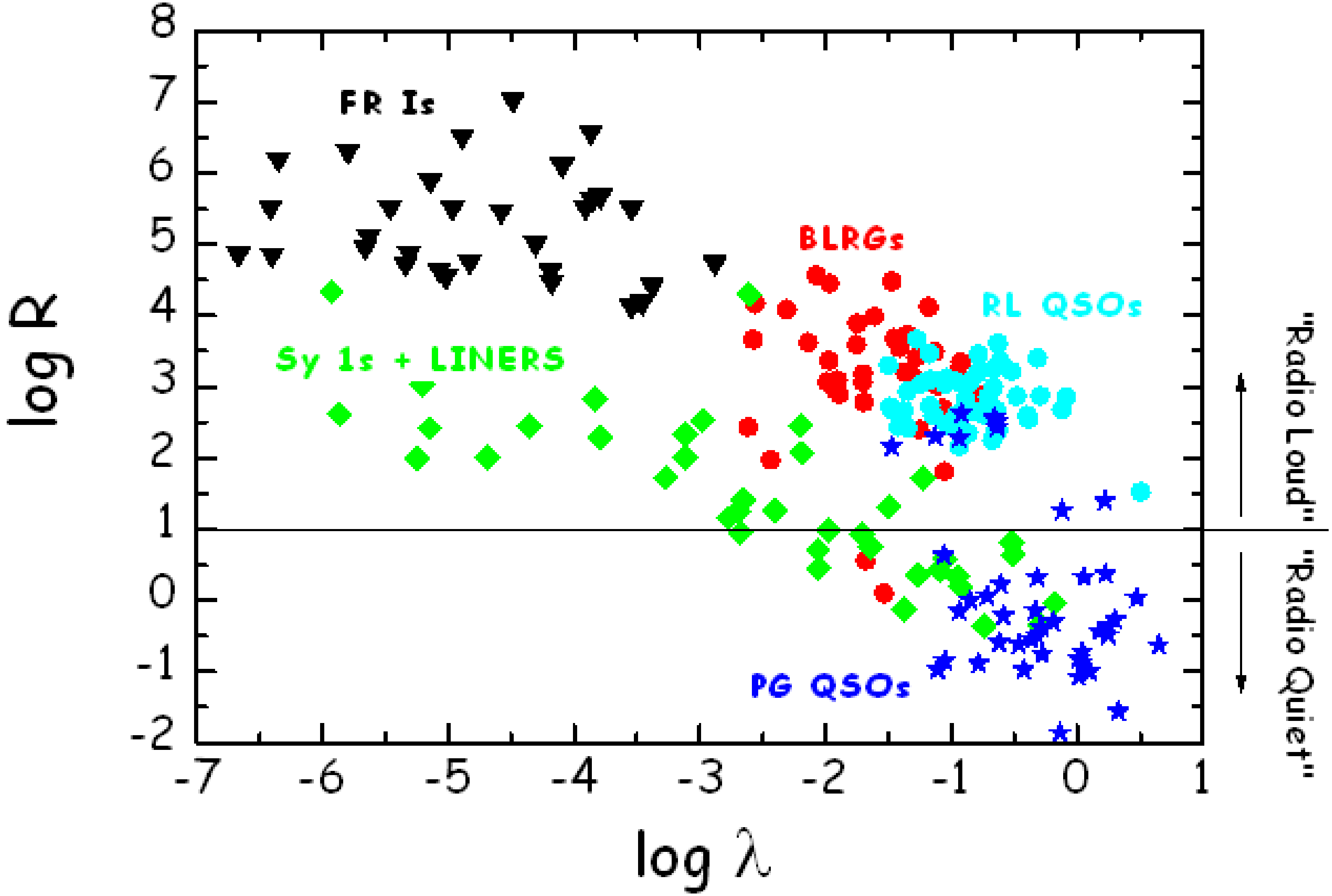

Sikora, Stawarz, & Lasota '07

(see also: Chiaberge et al. '05; Panessa et al. '07; Maoz '07)

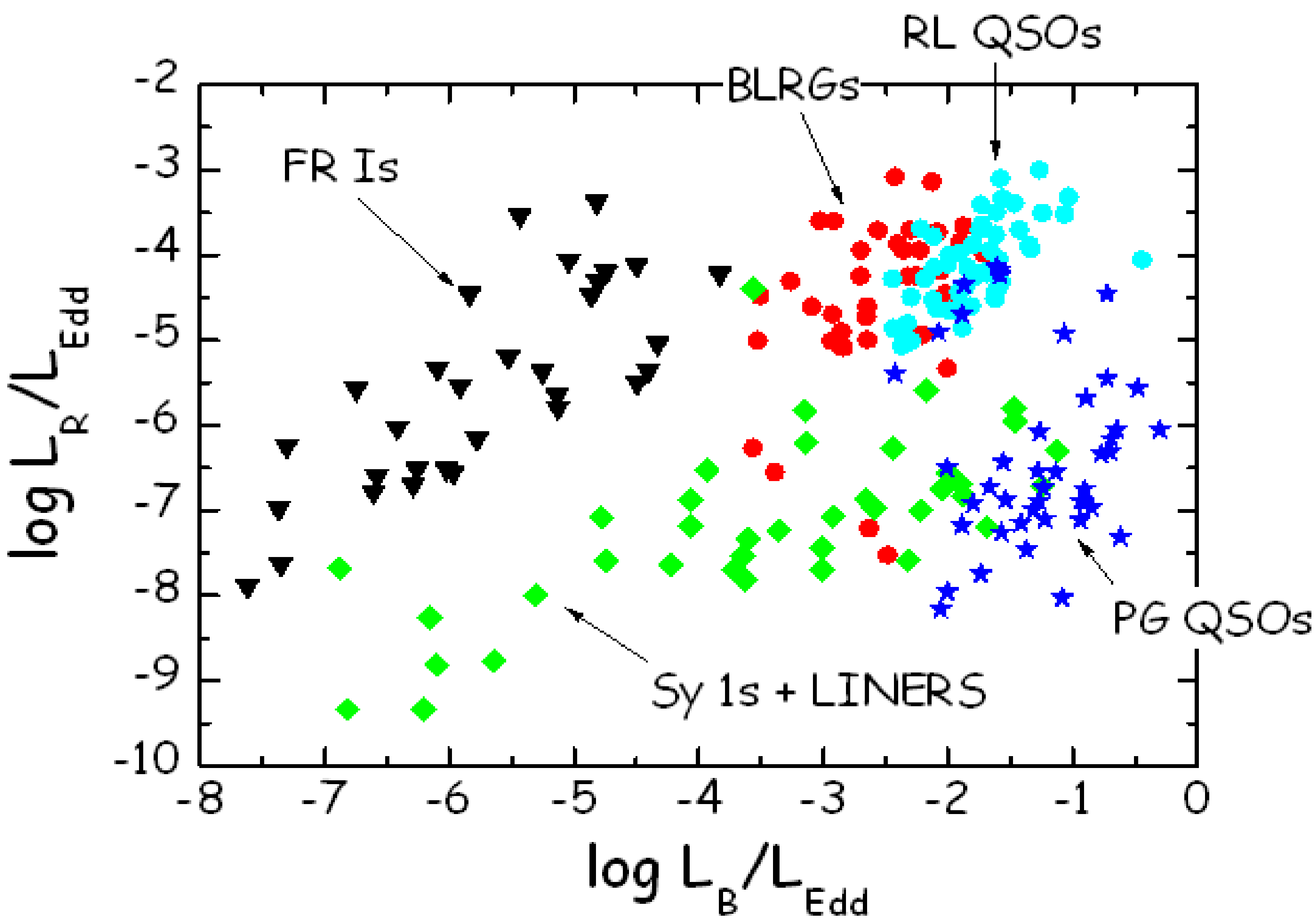

Sikora et al. '07

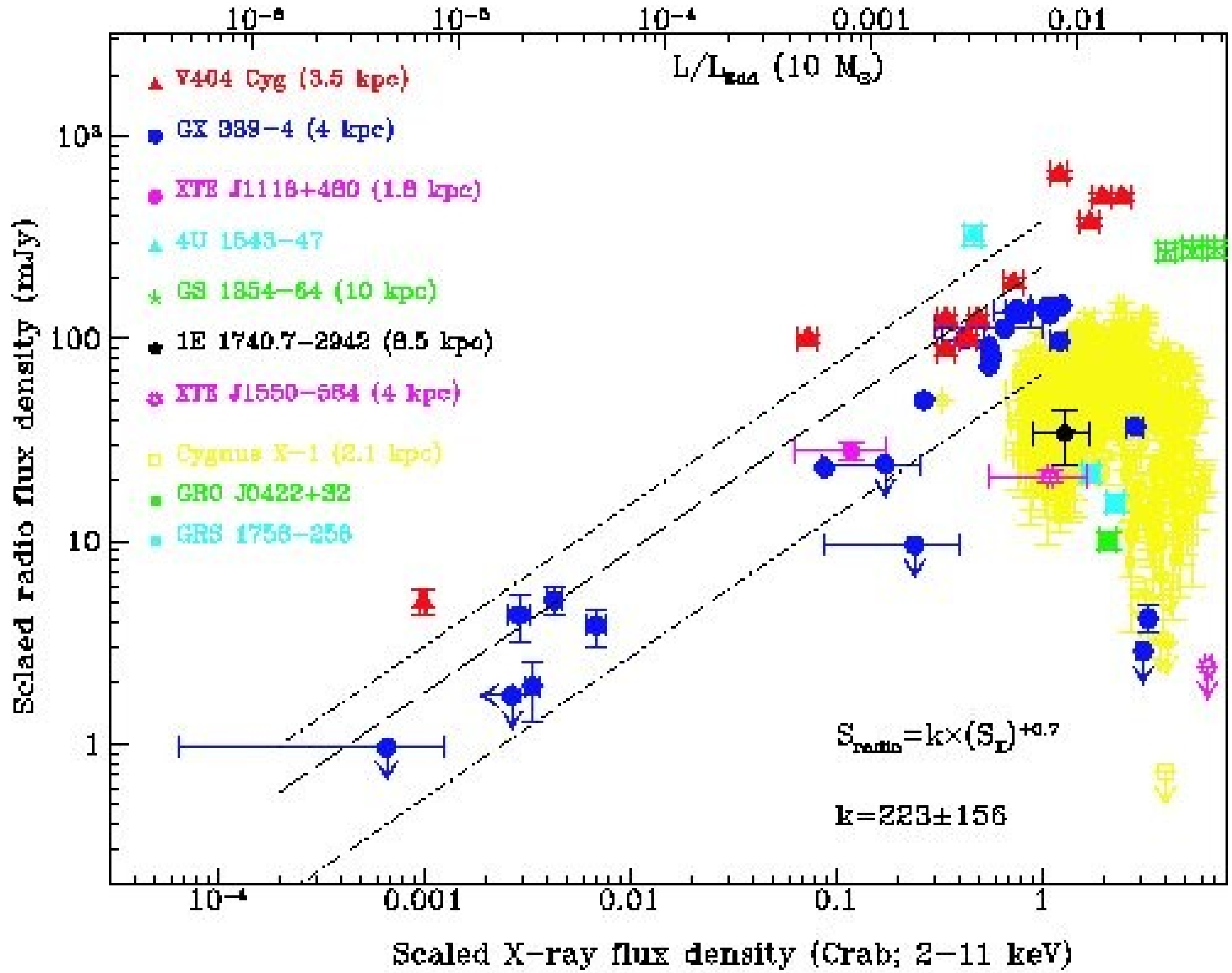

Figure 2. The radio flux density (mJy) is plotted against the X-ray flux density (Crab) for a sample of 10 hard state BHs (see Table 1), scaled to a distance of 1 kpc and absorption corrected (this means that the axes are proportional to luminosities). On the top horizontal axis we indicate luminosity, in Eddington units for a 10-$M_\odot$ BH, corresponding to the underlying X-ray flux density. An evident correlation between these two bands appears and holds over more than three orders of magnitude in luminosity. The dashed line indicates the best fit to the correlation, that is $S_{radio} = k(S_X)^{+0.7}$, with $k = 223 \pm 156$ (obtained by fixing the slope at +0.7, as found individually for both GX 339−4 and V404 Cygni; see Section 4.1). Errors are given at the 3σ confidence level and arrows also represent 3σ upper limits.

Gallo et al. '03

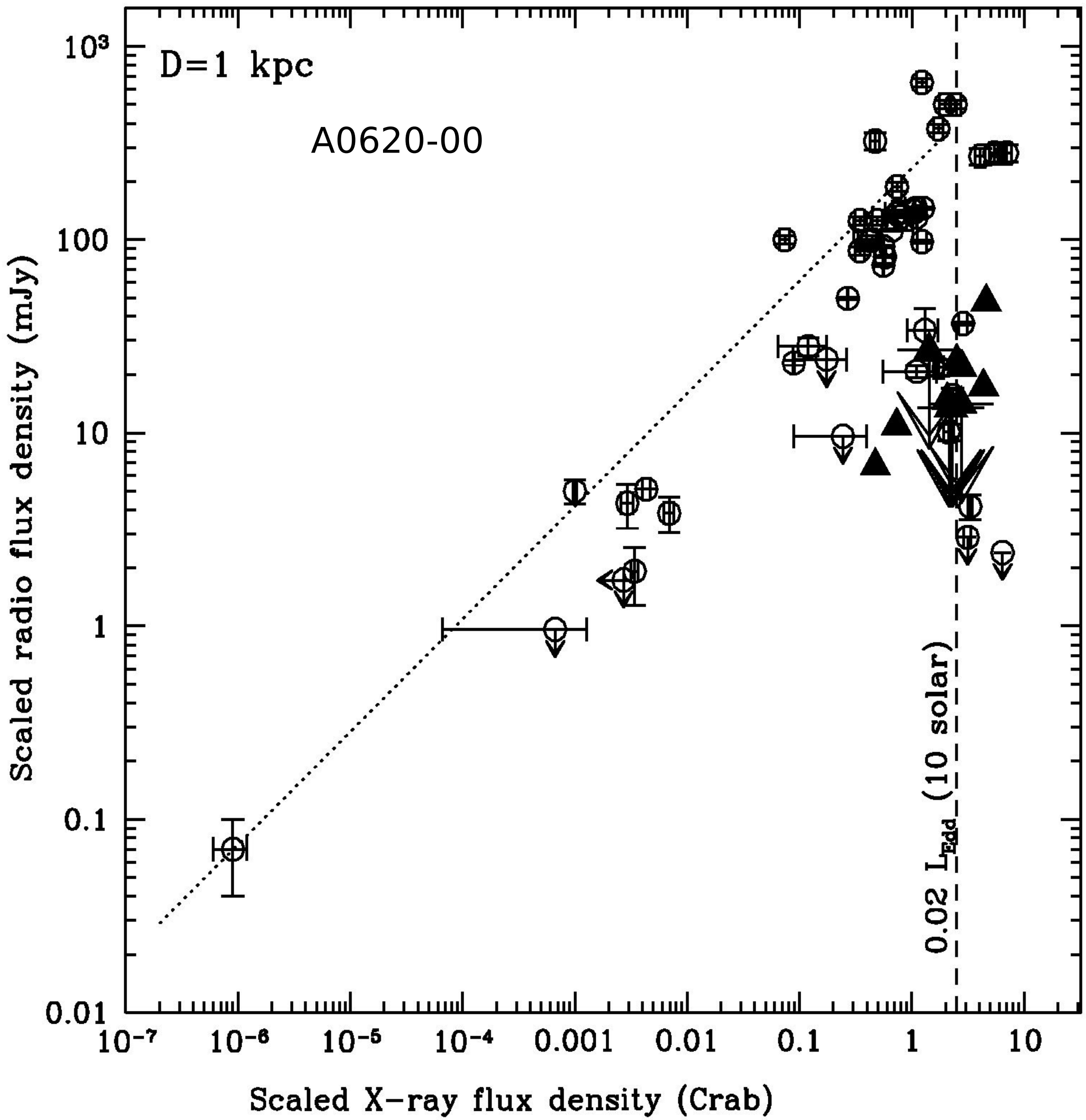
D=1 kpc
A0620-00
Scaled radio flux density (mJy)
Scaled X-ray flux density (Crab)
0.02 L$_{Edd}$ (10 solar)
10^3
100
10
1
0.1
0.01
10^{-7}
10^{-6}
10^{-5}
10^{-4}
0.001
0.01
0.1
1
10

Gallo '07

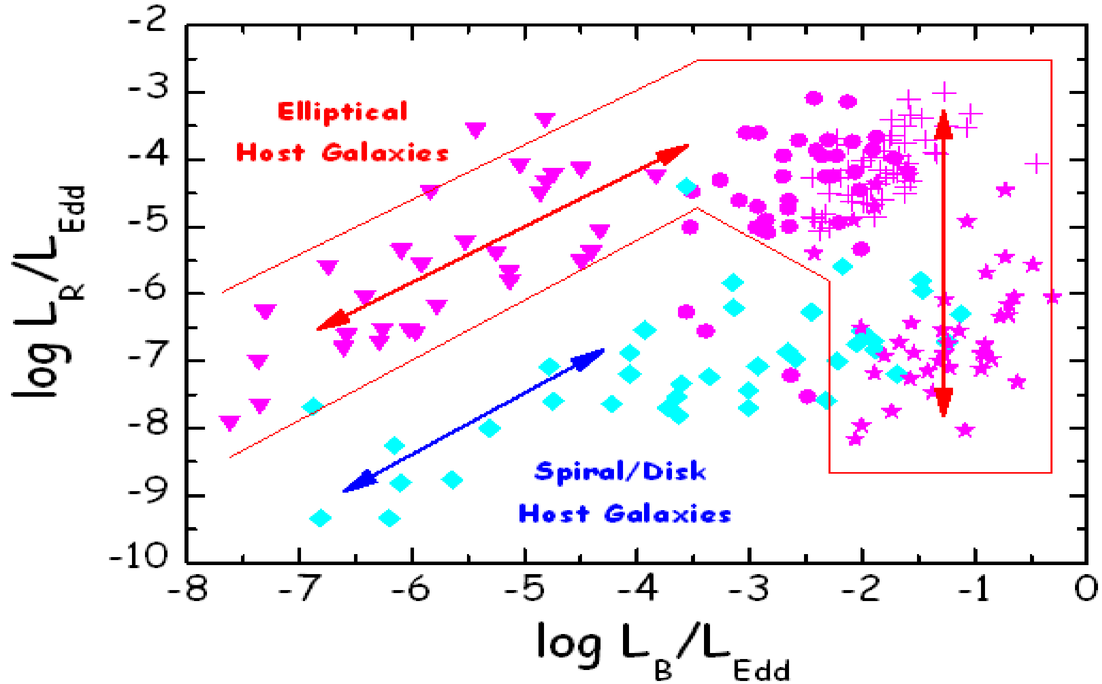
Elliptical
Host Galaxies
Spiral/Disk
Host Galaxies
log L_R/L_Edd
log L_B/L_Edd
-2
-3
-4
-5
-6
-7
-8
-9
-10
-8
-7
-6
-5
-4
-3
-2
-1
0

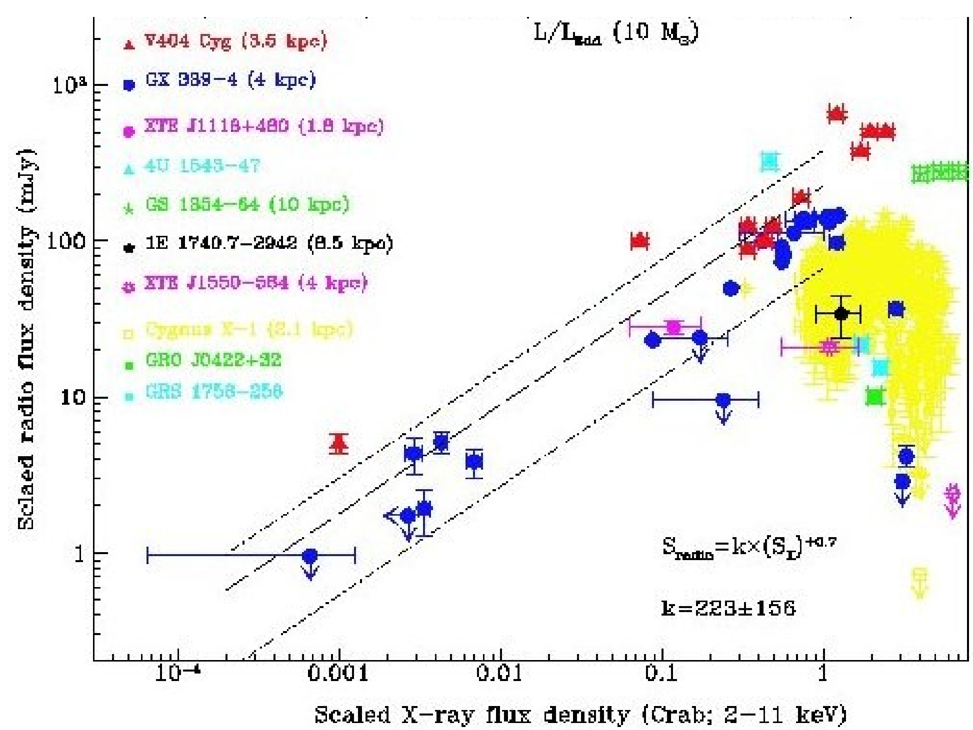
V404 Cyg (3.5 kpc)
GX 339-4 (4 kpc)
XTE J1118+480 (1.8 kpc)
4U 1543-47
GS 1354-64 (10 kpc)
1E 1740.7-2942 (8.5 kpc)
XTE J1550-564 (4 kpc)
Cygnus X-1 (2.1 kpc)
GRO J0422+32
GRS 1758-258
L/L_Edd (10 M_☉)
S_radio=k×(S_X)^+0.7
k=223±156
Sclaed radio flux density (mJy)
Scaled X-ray flux density (Crab; 2-11 keV)
10³
100
10
1
10⁻⁴
0.001
0.01
0.1
1

Jet production efficiency

- $\dot{m}$ + environment ? (e.g. Kauffmann et al. '07)
- $\dot{m}$ + topology of seed B ? (Beckwith, Hawley & Krolik '07)
- $\dot{m}$ + BH spin ? (Blandford '90 ; Wilson & Colbert '95)

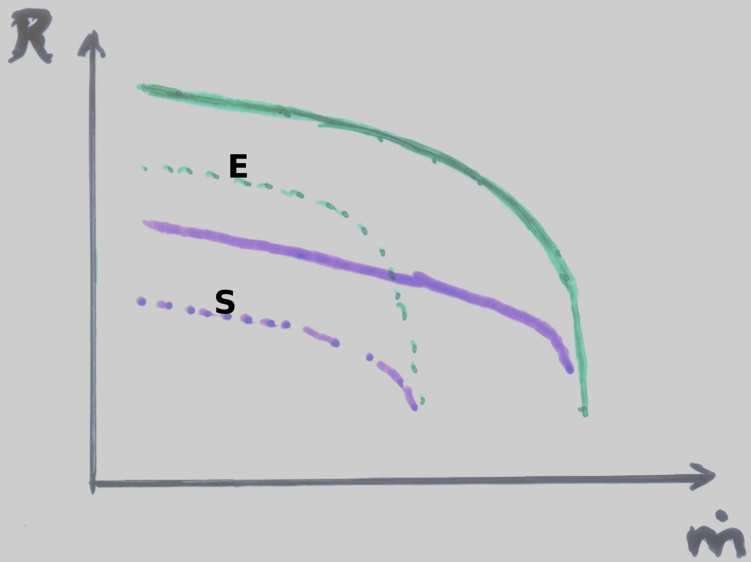

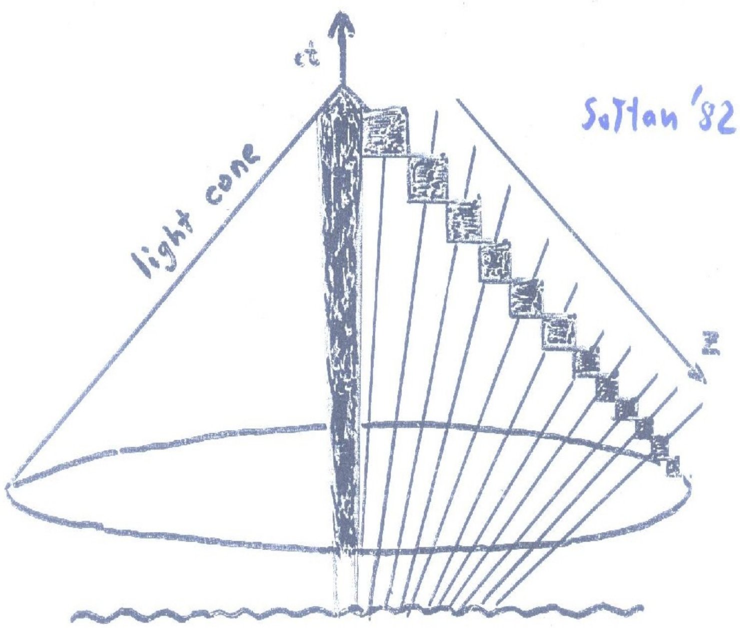

$$\eta_{rad,obs} = \frac{E - \Delta E}{M_h}$$

$$\eta_{rad,acc} = \frac{E}{M_h}$$

$$\boxed{\eta_{rad,acc} > \eta_{rad,obs}}$$

Yu & Tremaine '02
Elvis et al. '02
Gammie et al. '04
Wang et al. '06

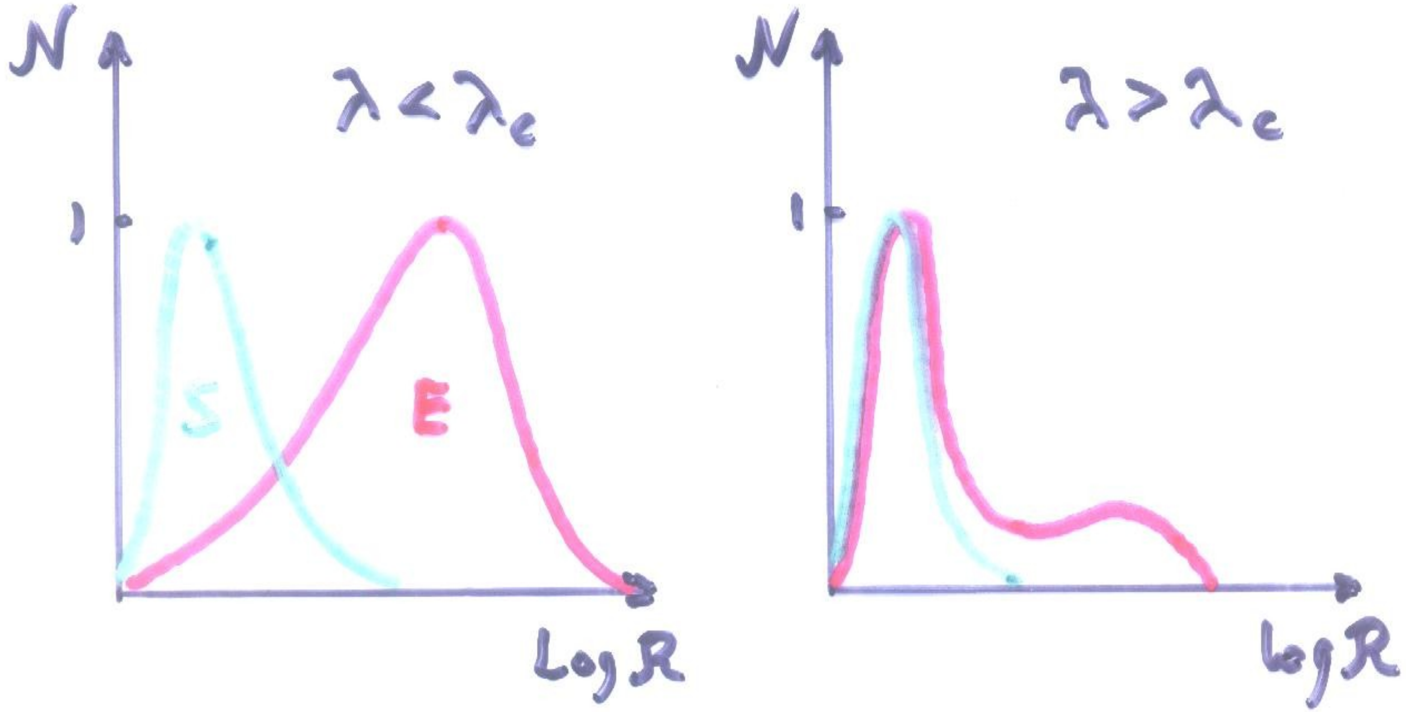

- Why BH have larger spins in Ellipticals than in Spirals?
- How to get switches between radio-loud and radio-quiet states?

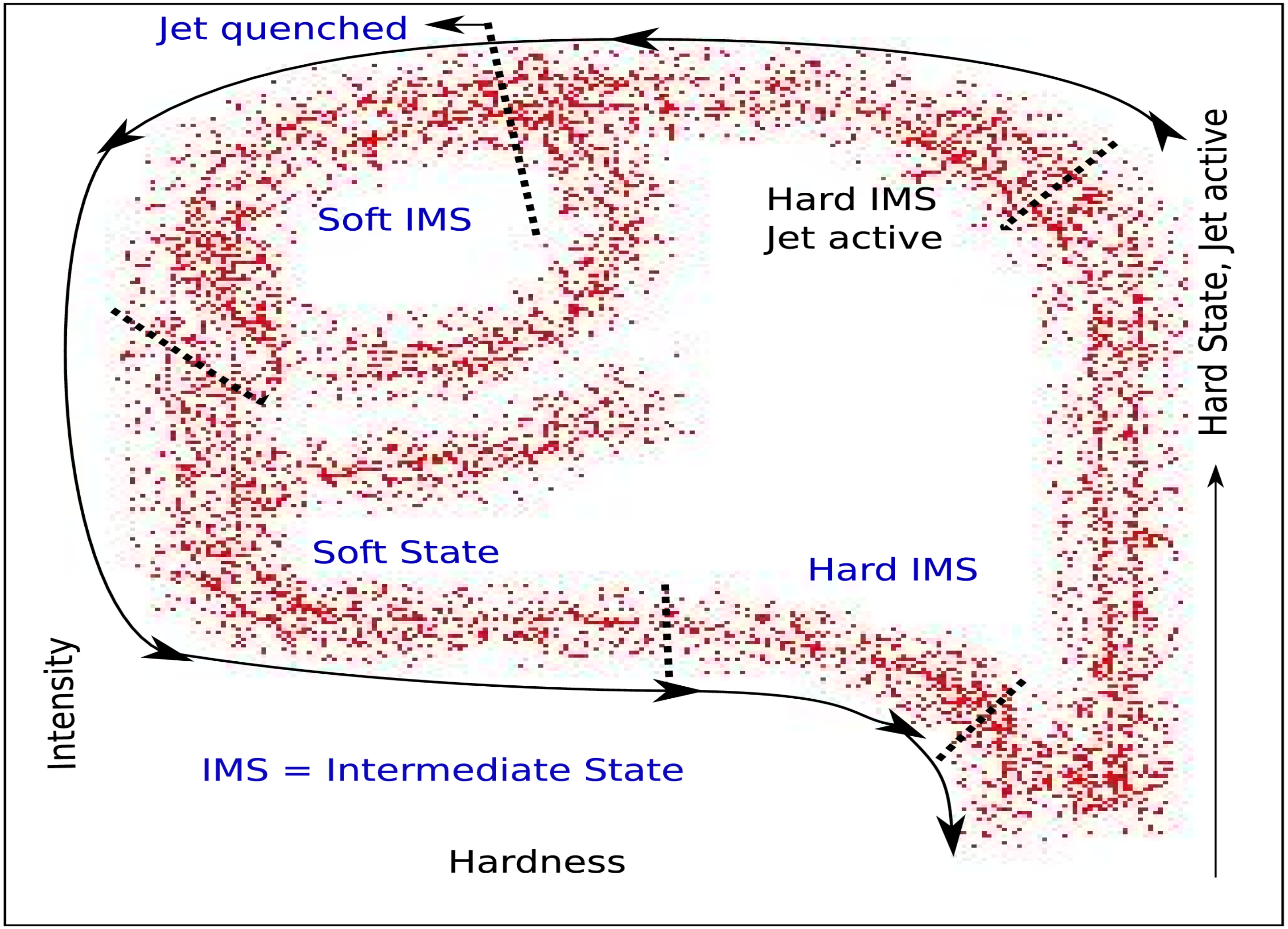

Kording et al. '06

Transitions between two accretion modes: *Livio et al. '03; Spruit & Uzdensky '05*

FRII radiogalaxy B0925+420

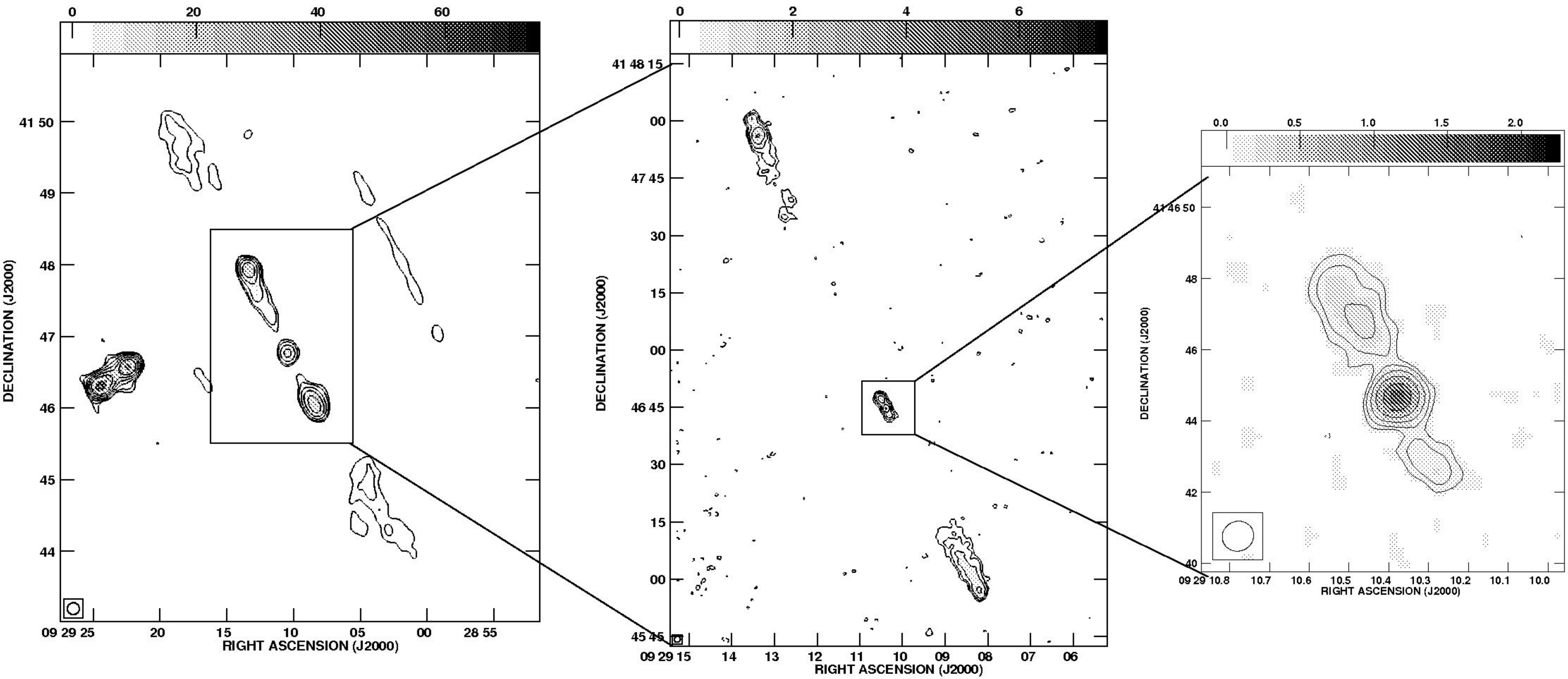

Brocksopp et al. '07

Relative Makeup of Quasar Sample

Quasar Group	Number	Fraction (%)
Quasars with detected cores (3 σ limit)................	5313	11.8
Non-FR2 quasars with detected cores..................	4766	10.6
FR2 quasars	749	1.7
FR2 quasars with detected cores..........................	547	73
FR2 quasars without cores	202	27
Total quasars	44984	...

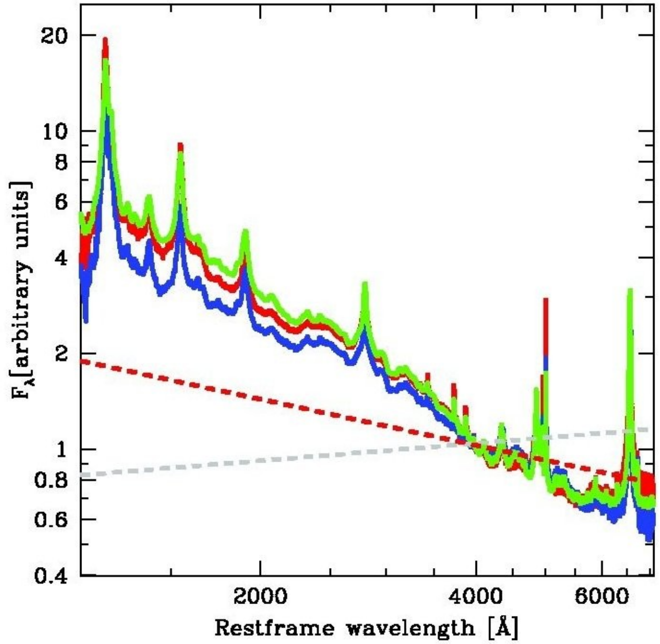

Fig. 7.—Composite spectra for our three samples of quasars: RQ (*green*), CD radio-loud (*blue*), and lobe-dominated (FR2) radio-loud (*red*). This plot can be directly compared to Fig. 7 of Richards et al. (2003), and it illustrates both the small relative color range among our three samples (all fall within the "normal" range of Richards et al.) and the apparent lack of significant intrinsic dust reddening in these quasars (the red and gray dashed lines represent moderate to severe levels of dust reddening). All spectra have been normalized to the continuum flux at 4000 Å.

De Vries, Becker & White '06

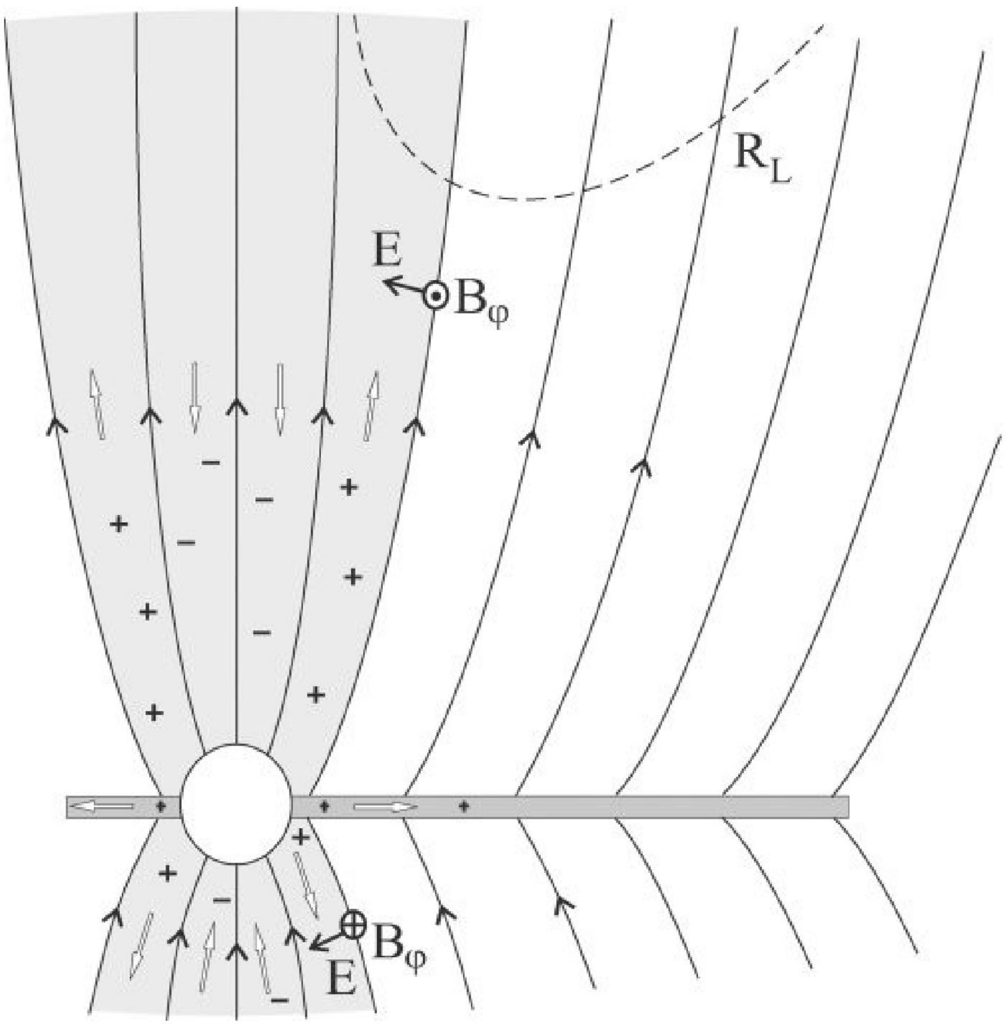

Beskin & Nokhrina '06

Others: Sol et al. '89; Bogovalov & Tsinganos '05; Gracia et al. '05

Spin Evolution

- BH mergers
- Accretion
- BZ mechanizm
- Lense-Thirring torque

Refs.: Lense & Thirring '18; Bardeen '70; Wilkins '72; Thorn '74; Bardeen & Petterson '75; Blandford & Znajek '77; Rees '78; Begelman, Blandford & Rees '80; Papaloizou & Pringle '83; Wilson & Colbert '95 Scheuer & Feiler '96; Moderski & Sikora '96,'97; Moderski, Sikora & Lasota '98; Natarajan & Pringle '98 Hughes & Blandford '03; Volonteri, Madau, Quataert & Rees '05; King, Lubow, Ogilvie & Pringle '05

Counter-rotation :

$$\left.\begin{aligned} \vec{J}_{tot} &= \vec{J}_h + \vec{J}_d = const \\ J_h &= const \Rightarrow J_d \searrow \end{aligned}\right\} \Rightarrow \boxed{\frac{J_d}{2J_h} < -\cos\theta}$$

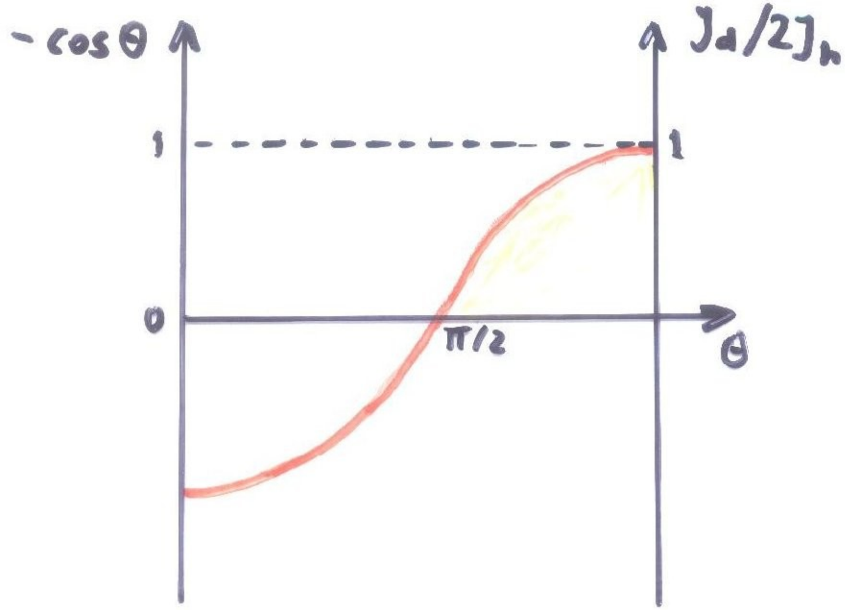

counter-alingment occurs in a fraction

$$f = \frac{1}{2}\left[1 - J_d/2J_h\right]$$

King et al. '06

$$J_h = \frac{J_h}{J_{h,max}} J_{h,max} = a\frac{GM_h^2}{c} = \sqrt{GM_h} \times aM_h\sqrt{R_h}$$

$$J_d \simeq I_d \Omega_K = m_d R_d^2 \sqrt{\frac{GM_h}{R_d^3}} = \sqrt{GM_h} \times m_d \sqrt{R_d}$$

$$J_d \ll J_h \rightarrow \frac{m_d}{M_h} \ll a\sqrt{\frac{R_h}{R_d}}$$

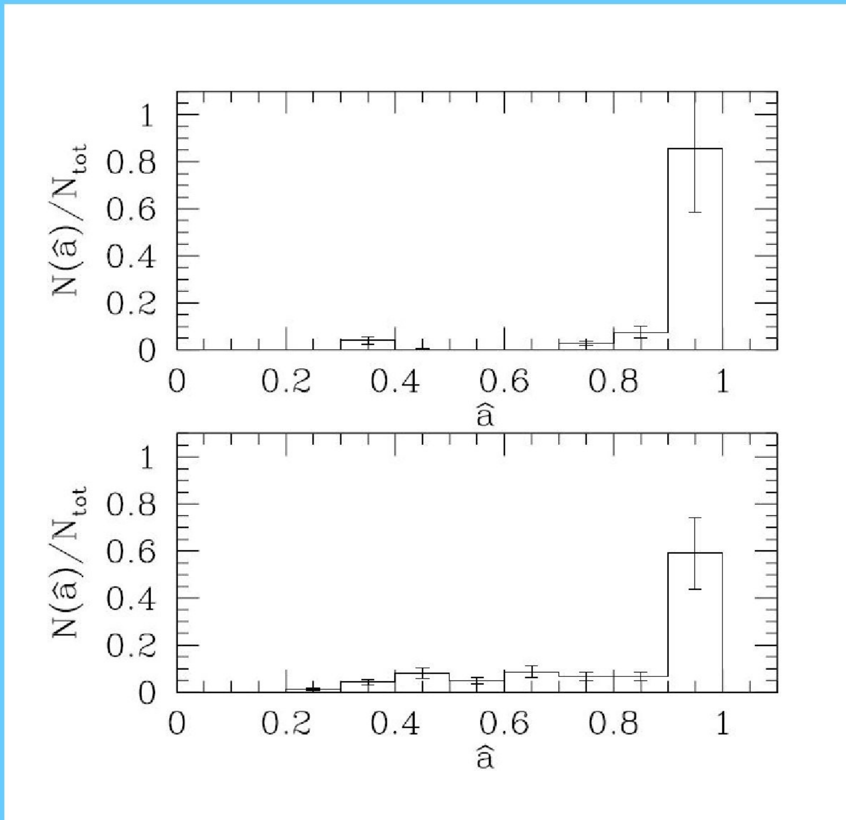

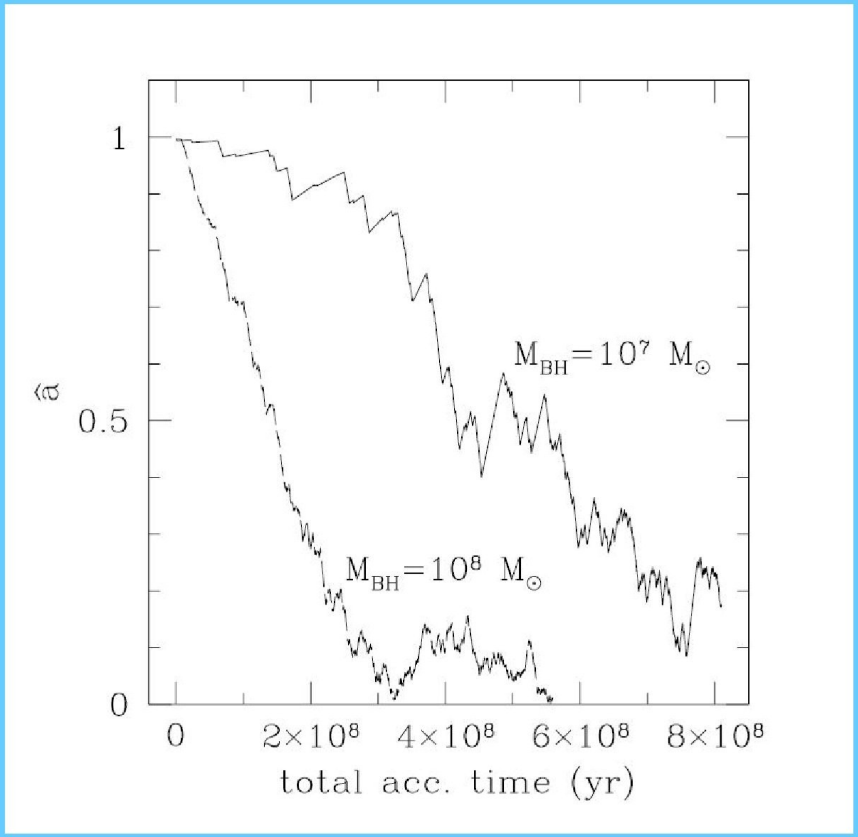

Spin of BHs at z=0 in elliptical (upper) and disc (lower) galaxies. BH grows by a sequence of randomly oriented accretion episodes in a merger driven scenario. Here, E/D classification is based on the frequency of major and minor mergers.

Evolution of BH spins due to accretion of molecular clouds cores. A lognormal distribution for the mass function of molecular clouds is assumed. Spin down in a random walk fashion is observed.

Volonteri, Sikora & Lasota 2007

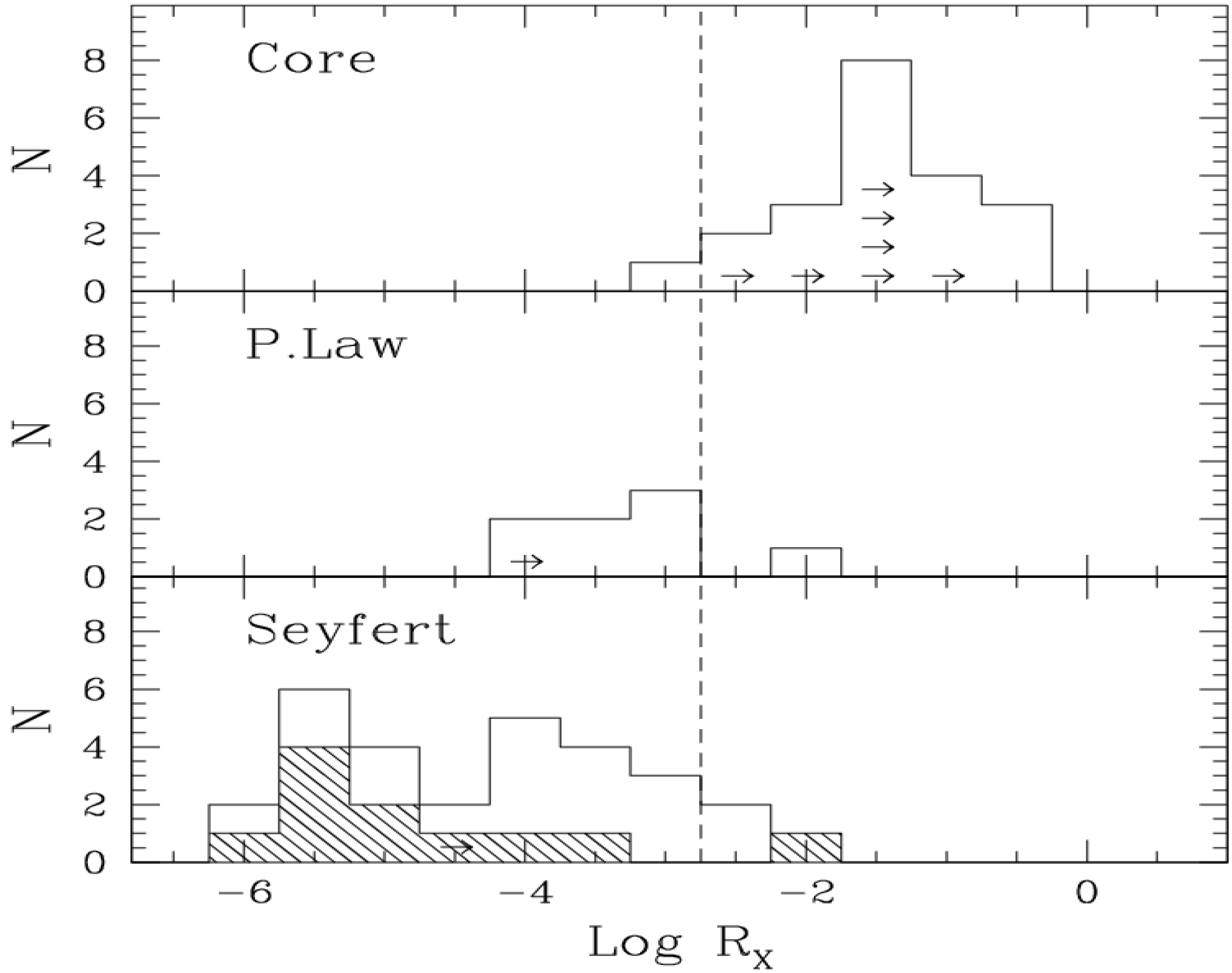

Capetti & Balmaverde '07

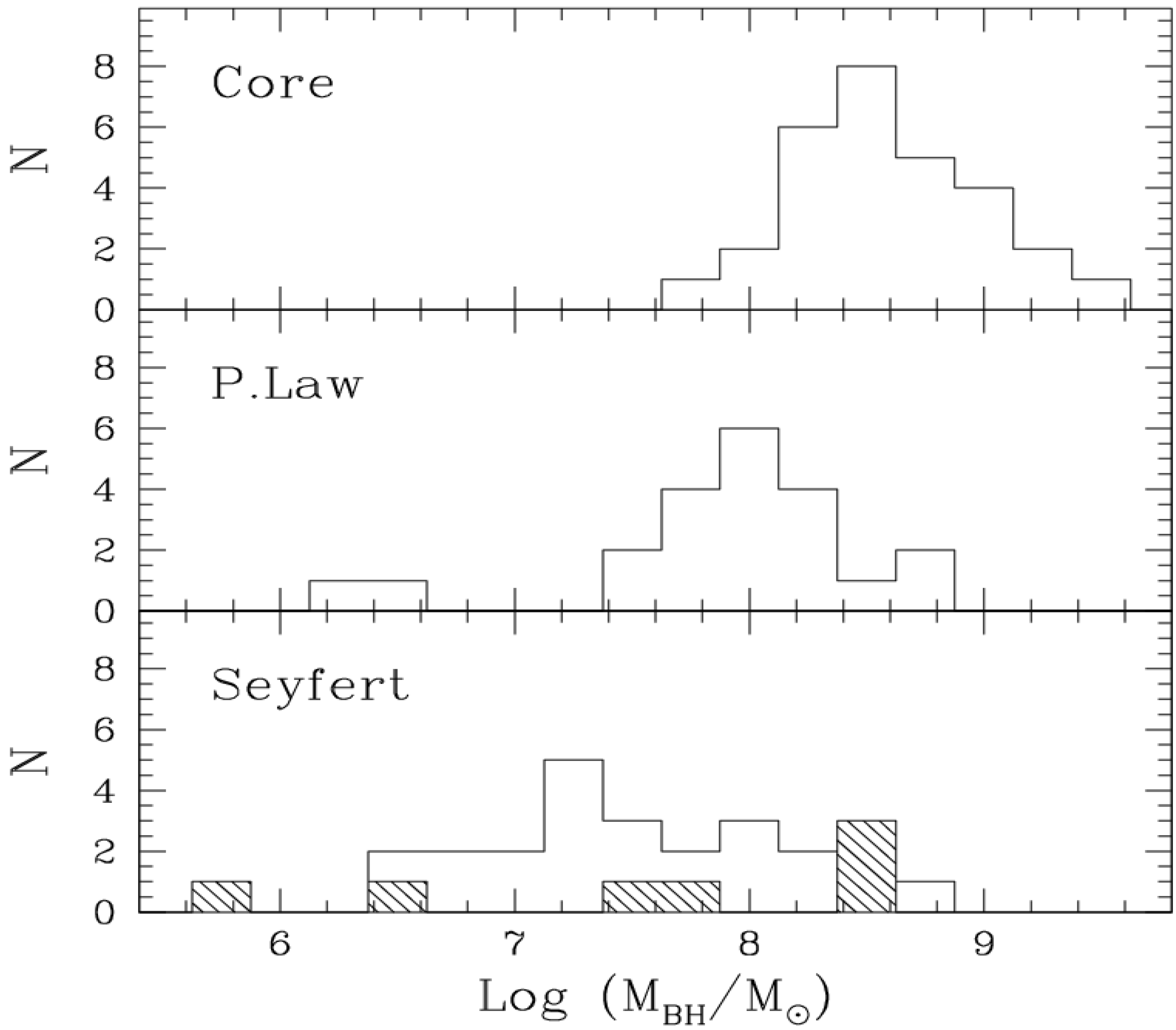

Capetti & Balmaverde '07

Conclusions

a) The upper boundaries of radio-loudness of AGNs hosted by giant elliptical galaxies are by ~3 orders of magnitude larger than upper boundaries of radio-loudness of AGNs hosted by disc galaxies.

b) Both populations of spiral-hosted and elliptical-hosted AGNs show a similar but distinct dependence of the upper bounds of the radio loudness parameter on the Eddington ratio (the radio loudness increases with decreasing Eddington ratio, faster at higher accretion rates, slower at lower accretion rates).

c) We propose that the huge, host-morphology-related difference between the radio-loudness reachable by AGNs in disc and elliptical galaxies can be explained by the scenario according to which the spin of a black hole determines the outflow's power, and central black holes can reach large spins only in early type galaxies (following major mergers), and not (in a statistical sense) in spiral galaxies.